A novel polysaccharide-grafted gold nanoparticles synthesized via carboxyl-trithiocarbonates for modification of separation membrane

Shaohu Zhang[2,b)], Xiaoqin Niu[1,b)], Qi Wang[2], Dan Li[2], Weijie Zhang[3], Yuhong Chen[1], Fen Ran[2,a)]

[1] College of Petrochemical Technology, Lanzhou University of Technology, Lanzhou 730050, Gansu, People's Republic of China
[2] State Key Laboratory of Advanced Processing and Recycling of Non-Ferrous Metals, School of Material Science and Engineering, Lanzhou University of Technology, Lanzhou 730050, Gansu, People's Republic of China
[3] School of Life Science and Engineering, Lanzhou University of Technology, Lanzhou 730050, Gansu, People's Republic of China
a) Address all correspondence to this author. e-mail: ranfen@lut.edu.cn ranfen@163.com
b) Dr. Xiaoqin Niu and Shaohu Zhang have contributed equally to this work

Permeability and selectivity are two important parameters for evaluating membrane separation performance. In this work, the polysaccharide-functionalized gold nanoparticles (DexDTM-AuNP) are synthesized by one-step reduction with NaBH$_4$ and used as additive for modification of PES membrane to improve the hydrophilicity of the membrane. In comparison with the pristine PES membrane, the water contact angle (WCA) of the DexDTM-AuNP-modified membrane significantly decreases. When the content of DexDTM-AuNP is 3 wt%, the WCA of the modified membrane decreases from 89.3° to 61.1°, indicating excellent hydrophilicity. The modified membrane shows high pure water flux of up to 134.5 L m^{-2} h^{-1}, and the rejection ratio for bovine serum albumin, congo red, and methyl blue are 98.8, 99.3, and 93.6%, respectively. DexDTM-AuNP-modified membrane exhibits excellent hydrophilicity, anti-fouling ability, and separation performance. Therefore, the strategy has great potential for practical applications in water purification and other separation fields.

Introduction

With the progress of society and the continuous development of industrialization, environmental pollution has become increasingly serious, especially water pollution [1, 2]. In general, domestic wastewater and industrial wastewater are important sources of water pollution [3]. These wastewaters often contain large amounts of proteins/bacteria and oils. If they are directly discharged, they will cause serious environmental pollution and aggravate the water crisis [4–6]. Contaminated water contains pathogenic microorganisms that may cause waterborne diseases through direct contact or oral administration [7–9]. Therefore, it is particularly important to efficiently treat these wastewaters containing bacteria and oil, and it has gradually become an important research area involving environmental, economic, and social issues [10, 11]. Membrane separation technology has become the preferred technology in the field of water treatment [12–14].

In recent years, the application of polymer membrane separation technology in the field of water treatment has received increasing attention [15, 16]. Compared with traditional separation technologies (distillation and extraction), polymer membrane separation technology has the advantages of high separation efficiency, no phase change in the separation process, separation at room temperature, small footprint, and simple operation [17–19]. The most commonly used polymer membrane materials are polyethylene, polypropylene, polyvinylidene fluoride, polysulfone, and polyethersulfone [20–22]. Among many polymer membrane materials, polyethersulfone (PES) is widely used in the field of water treatment due to its excellent mechanical properties, good thermal stability, excellent chemical stability, and excellent membrane forming properties [23, 24]. However, PES membrane still has problems in water treatment. On the one hand, due to the strong hydrophobicity of PES, the water flux of the membrane is low in the filtration

process. On the other hand, PES membrane has poor anti-fouling performance, which is easy to absorb organic pollutants such as proteins [25, 26]. During the filtration process, it is easy to be polluted by proteins and other organic substances in the water, resulting in the membrane pore being blocked and the water flux seriously decreasing. Therefore, how to improve the water flux and anti-fouling performance of PES membranes is a research hotspot in the field of membrane separation [27, 28]. Hydrophilic modification of PES membrane is the most effective method to improve the permeation flux, separation performance and anti-fouling performance of PES membrane.

Currently, widely used polymer membrane modification methods include physical methods and chemical methods [29, 30]. In the physical modification method, the polymer monomer used to prepare the separation membrane does not undergo chemical reaction, and the physical modification method includes blending modification and surface coating modification [31, 32]. However, in the chemical modification method, the polymer monomers for preparing the separation membrane undergo a chemical reaction. And common chemical methods for membrane modification include interfacial polymerization modification, bulk modification, graft modification, and plasma modification. Among these modification methods, blending is the simplest and most commonly used membrane modification method [33, 34].

The blending modification of the PES membrane is to blend a hydrophilic polymer or functionalized nanoparticles with PES and prepare a modified membrane by a phase inversion method [35, 36]. Blending modification has the following advantages: modification and membrane formation are carried out simultaneously, the process is simple, and no complicated subsequent processing steps are required; the modifier can cover the membrane surface and the inner wall of the membrane pores at the same time and will not damage the structure of the membrane [37, 38]. For example, the introduction of an appropriate amount of hydrophilic additives not only improves the mechanical strength of the composite membrane but also greatly improves its hydrophilicity, which has better anti-fouling ability. The additives commonly used in PES blend modification currently include inorganic nanoparticles, hydrophilic polymers, amphiphilic polymers, etc. [39, 40].

In this study, the polysaccharide-functionalized gold nanoparticles (DexDTM-AuNP) are synthesized by one-step reduction with $NaBH_4$ and used as additive for modification of PES membrane to improve the hydrophilicity of the membrane. First, dextran-based macromolecular chain transfer agent (DexDTM) was synthesized via esterification of 2-(dodecylthiocarbonothioylthio)-2-methylpropanoic acid (DTM) with the hydroxyl groups of dextran. Subsequently, the dextran-based macromolecular chain transfer agent and the gold nanoparticles were combined together by Au–S bond

using a one-step reduction method of $NaBH_4$ to prepare a polysaccharide-functionalized gold nanoparticle. As a natural polysaccharide, dextran has excellent biocompatibility, excellent hydrophilicity, and anti-fouling properties. And gold nanoparticles have an effective inhibitory effect on bacteria, fungi, and other microorganisms in water. Grafting dextran onto gold nanoparticles can combine the advantages of gold nanoparticles and polysaccharides to obtain complementary functions. When DexDTM-AuNP is blended with PES to prepare a modified membrane by phase inversion, the hydrophilic segments in the DexDTM-AuNP will spontaneously migrate to the membrane surface and be enriched on the membrane surface, which makes the hydrophilicity of the modified membrane significantly improved.

Results and discussion

The polysaccharide-functionalized gold nanoparticles are synthesized by one-step reduction with $NaBH_4$, as shown in Scheme 1. Briefly, 2-(dodecylthiocarbonothioylthio)-2-methylpropanoic acid (DTM) is esterification reacted with dextran hydroxyl group to synthesize dextran-DTM (DexDTM). Subsequently, DexDTM is used as nucleating agent and stabilizing agent, and chloroauric acid as gold precursor is dissolved in deionized water in order. After being stirred in an ice-water bath for 30 min, the strong reducing agent $NaBH_4$ is added to reduce the trithiocarbonyl group in DexDTM to a mercapto group and reduce the chloroauric acid to gold nanoparticles (AuNP). Then, the gold nanoparticles and the mercapto group in DexDTM self-assemble form Au–S bond to obtain the DexDTM-functionalized gold nanoparticles (DexDTM-AuNP). Grafting hydrophilic polymer chains of DexDTM to gold nanoparticles can significantly improve the hydrophilicity and dispersibility of gold.

^{1}H-NMR spectrum of DexDTM is displayed in Fig. 1a. It can be observed that there are two chemical shifts at 1.24 and 1.03 ppm, which attribute to -CH_3 (H-*a* and H-*b*). The peaks distributed in 3.17–3.77 ppm belong to the H-*c* of dextran. In addition, the peaks in 4.46–4.92 ppm ascribe to -OH (H–*d*). Figure 1b shows FTIR spectra of DexDTM and DexDTM-AuNP. The strong and wide absorption peak at 3397.9 cm^{-1} is caused by the stretching vibration of O–H group from dextran, while the peak at 2921.6 cm^{-1} attributes to the asymmetric stretching of C–H bond of –CH_2 group. The peak at 1031.7 cm^{-1} belongs to the O–H group angular vibration of dextran. The results of FTIR and ^{1}H-NMR characterizations confirm that DexDTM is successfully synthesized by esterification reaction of dextran and DTM. In addition, it can be seen from the FTIR spectra that the peak positions of DexDTM and DexDTM-AuNP have a high degree of matching, demonstrating that DexDTM is successfully grafted onto AuNP.
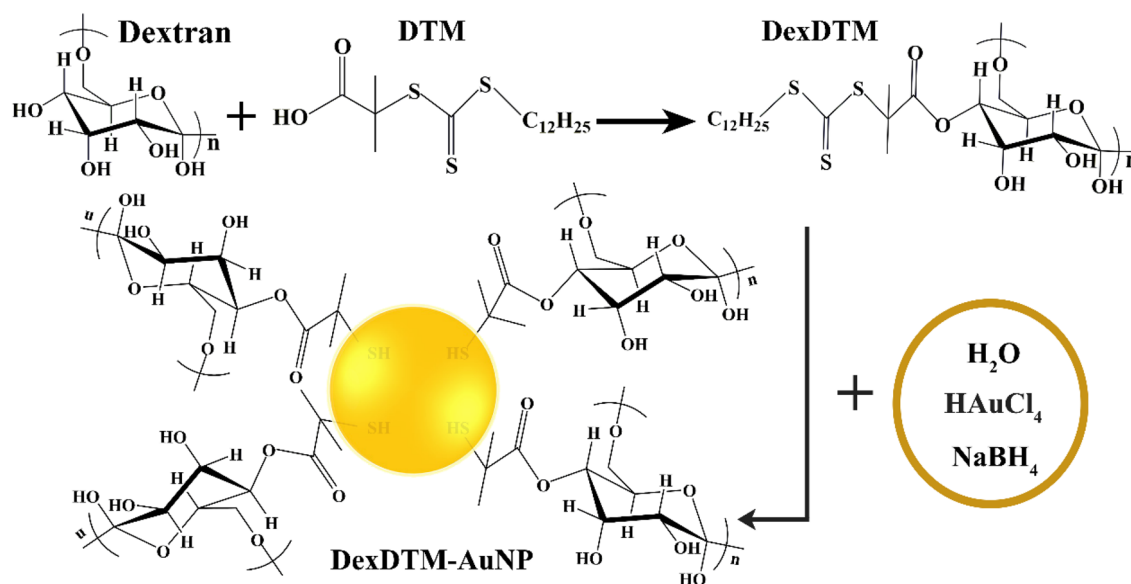
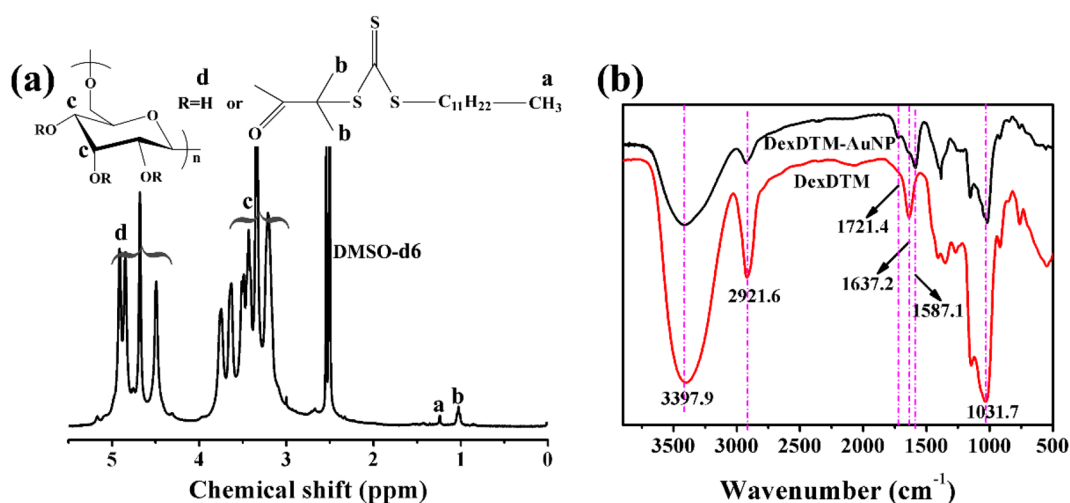**Scheme 1:** Synthesis process of DexDTM-AuNP.

Figure 1: (a) ^{1}H-NMR spectrum of DexDTM, and (b) FTIR spectra of DexDTM and DexDTM-AuNP.

The functionalized gold nanoparticles are fabricated and further used as additive for modification of PES membrane by blending method. The morphology of DexDTM-AuNP is characterized by TEM as shown in Fig. 2. It can be observed that the functionalized gold nanoparticles are uniform in size, uniformly distributed, and there is no agglomeration. Among them, Fig. 2b is a partial enlarged view of Fig. 2a. It can be seen that DexDTM-AuNP has a granular structure with a size of about 5 nm. DexDTM is connected to the gold particles through Au–S bonds, which can significantly improve the hydrophilicity and dispersibility of Au nanoparticles. Therefore, DexDTM-AuNP as an additive for PES membrane modification will be uniformly

distributed in the membrane matrix, which can greatly improve the hydrophilicity of the membrane.

The functional groups introduced on the surface of PES membrane are investigated by FTIR as shown in Fig. 3. From the FTIR spectra, it can be found that all membranes show the characteristic peaks at 1, 151.2 and 1, 298.2 cm^{-1} assigned to symmetric and asymmetric $O=S=O$ stretching vibrations of PES. The band at 1, 243.1 cm^{-1} can be attached to the asymmetric C–O–C stretching vibration of the PES substrate. Moreover, three new bands presented at 3, 400.3, 2, 928.5, and 1, 040.6 cm^{-1} in the spectrum of the DexDTM-AuNP-modified membrane, which attribute to O–H stretching vibration, C-H
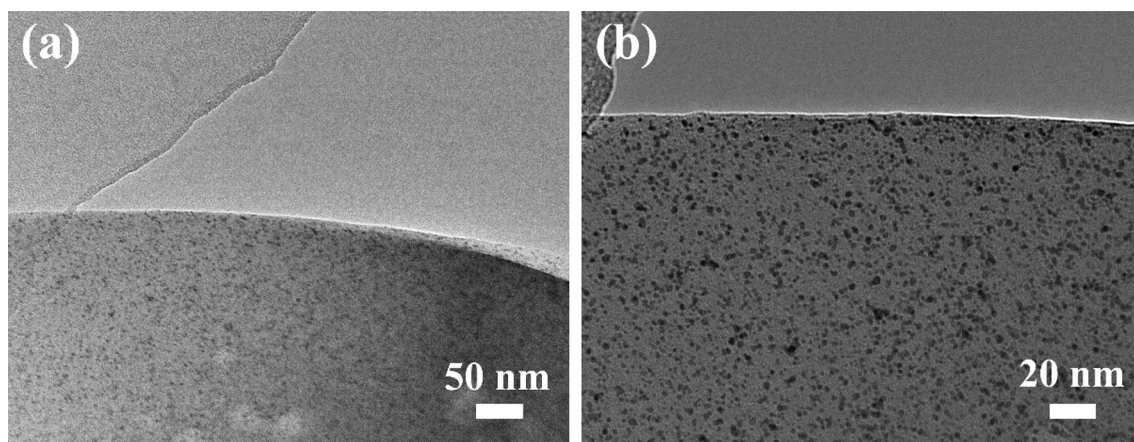
Figure 2: TEM images of DexDTM-AuNP with different magnifications and (b) is 2.5 times of (a).
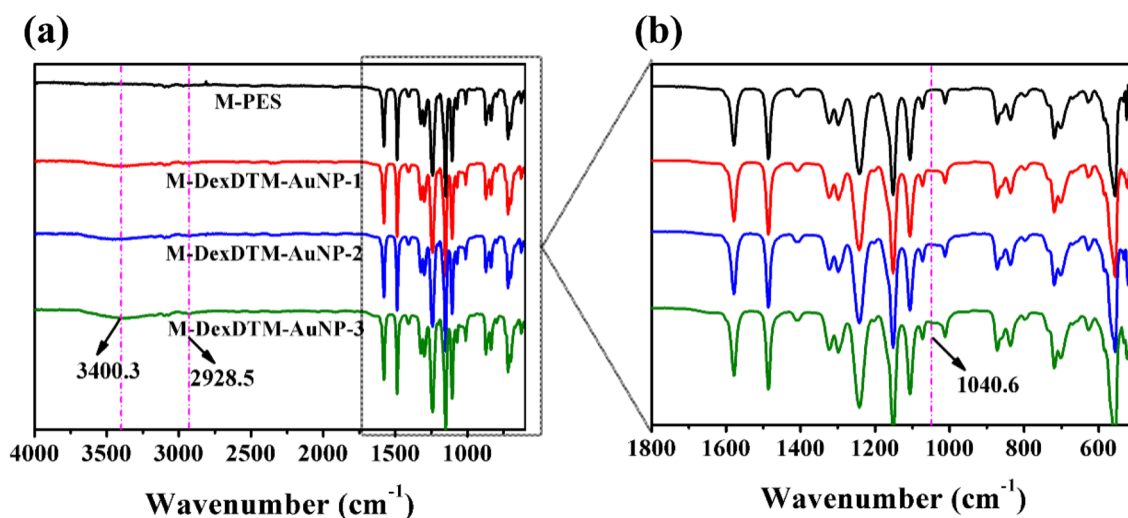
**Figure 3:** FTIR spectra for the modified membranes.

asymmetric stretching, and O–H angular vibration in DexDTM-AuNP. The results demonstrate that DexDTM-AuNP has been successfully introduced into the modified membrane.

Figure 4 shows the top surface morphology and structure of the membranes characterized by SEM at different magnifications. It can be seen that the surface of the pristine PES membrane is relatively flat and smooth. When DexDTM-AuNP is used as additive to blend to PES membrane, the surface morphology of the modified membrane becomes denser and the overall morphology changes little. As the content of DexDTM-AuNP further increases, uniformly distributed fine particles appear on the surface of the modified membrane, and the amount increases with the increase of the amount of the modifier. The main reason is that when the casting solution is immersed in the coagulation bath for phase conversion into a membrane, the hydrophilic segments in the modifier will

migrate to the surface of the membrane and enrich on the surface of the membrane, forming a hydrophilic molecular brush structure. However, the hydrophobic segment dodecyl in the modifier has excellent compatibility with the substrate membrane molecule, which can significantly improve the stability of the modifier in the membrane. The hydrophilic molecular brush enriched on the surface of membrane can significantly improve the hydrophilicity, anti-fouling ability, and permeability of the modified membrane.

The surface chemical compositions of the membranes were investigated by XPS. Figure 5 shows the XPS spectra of the upper surface of modified membrane with DexDTM-AuNP-3. As shown in Fig. 5a, the surface of the modified membrane contains C, O, S, and Au elements. The C 1 s peaks are shown in Fig. 5b, and the spectra are fitted into three peaks; a major peak is located at 284.7 eV ascribed to C–C/C–H bonds, an
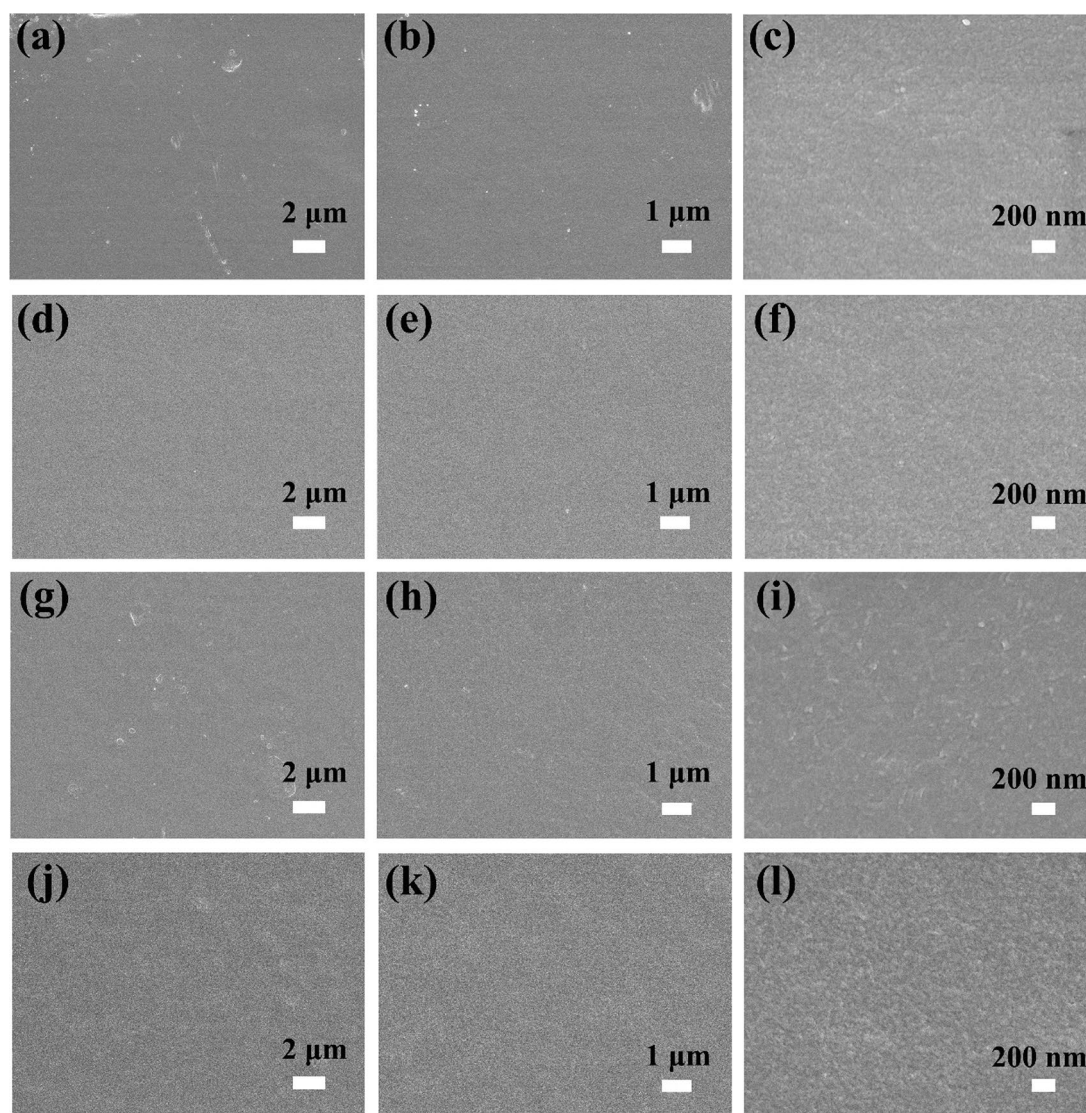
Figure 4: SEM images of the prepared membrane surface: (a, b, and c) M-PES, (d, e, and f) M-DexDTM-AuNP-1, (g, h, and i) M-DexDTM-AuNP-2, and (j, k, and l) M-DexDTM-AuNP-3.

intermediate peak appeared at 286.4 eV ascribes to C–O bond, and a minor peak at 291.5 eV corresponds to the C–S bond. The S 2p peaks as shown in Fig. 5c and the peaks at 167.4 and 168.4 eV belong to the S–O bond, and a minor peak at 163.2 eV attributes to S–Au bond. And from Fig. 5d, the binding energy of 83.4 eV corresponds to the Au $4f_{7/2}$, while the other located at 87.0 eV is attributed to the Au $4f_{5/2}$. The XPS spectra results further prove that DexDTM-AuNP has been successfully introduced into the modified membrane.

The surface chemical composition of the modified membrane and the elemental distribution in the membrane matrix are further confirmed by EDS mappings. EDS mappings on the upper surface of DexDTM-AuNP-3-modified membrane are shown in Fig. 6. It can also be observed that the modified membranes contain C, O, S, and Au elements. The figure shows that

Au evenly distributes on the surface of the modified membrane, demonstrating that DexDTM-AuNP are uniformly distributed in the modified membrane. Therefore, grafting DexDTM to gold particles through Au–S bond can significantly improve the stability and dispersibility of gold nanoparticles. The uniform distribution of DexDTM-AuNP on the surface of the modified membrane will greatly improve the hydrophilicity and anti-fouling ability of the modified membrane surface.

Figure 7 illustrates the cross-sectional morphologies of pristine and modified PES membranes. It can be observed that the cross-sectional images of all the membranes exhibit asymmetric finger-like porous structure similar to the most modified membranes prepared by NIPS method. The cross section of the modified membrane can be roughly divided into two parts: the top of the membrane cross section is a dense skin layer that acts as a
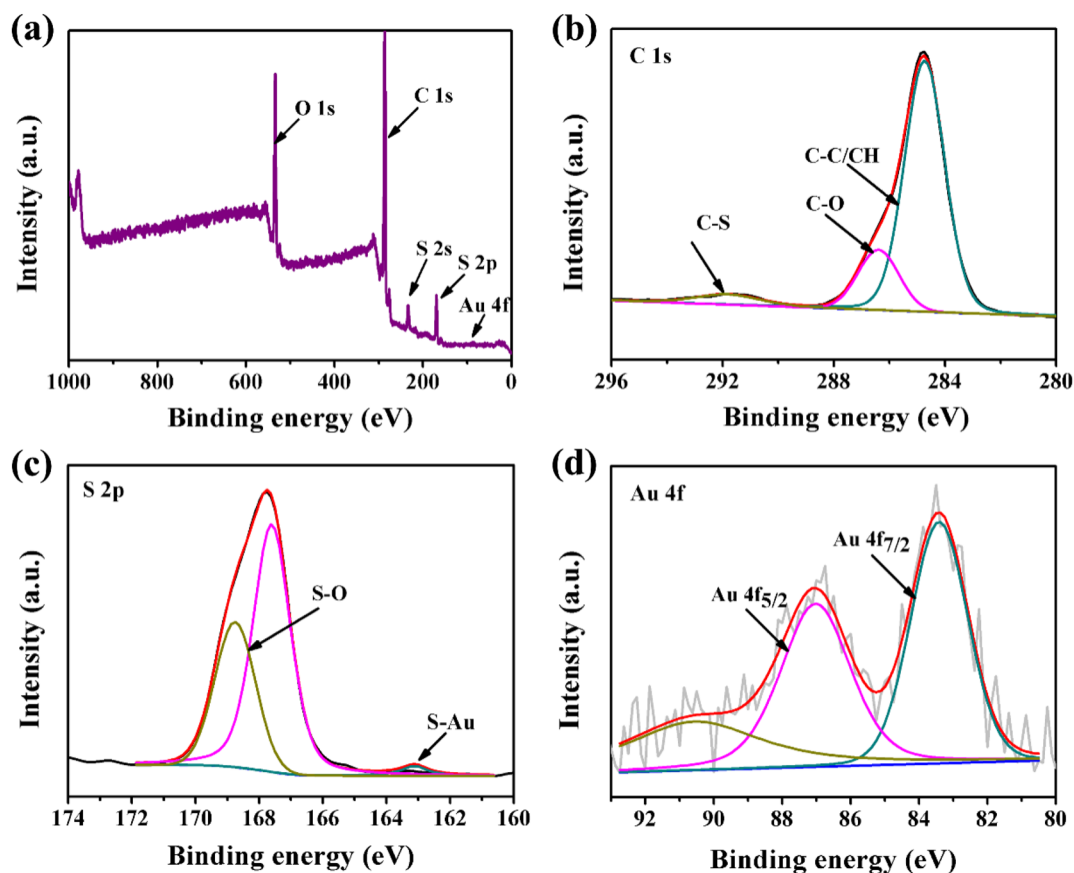
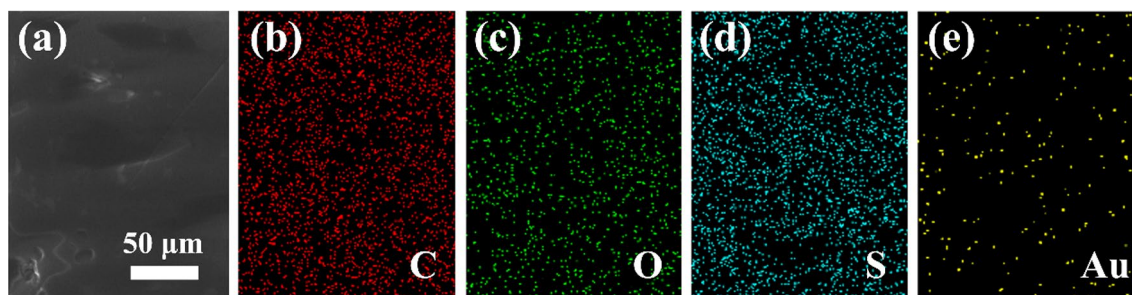**Figure 5:** XPS spectra of the upper surface of M-DexDTM-AuNP-3.

Figure 6: EDS mapping of M-DexDTM-AuNP-3 surface.

selective barrier, while the middle and bottom are thicker finger-like pore structures with a better mechanical strength. Compared with the pristine PES membrane, the finger-like pores in the cross section of the modified membrane become wider and increases with increase of DexDTM-AuNP content. The main reason for this phenomenon is mainly because the hydrophilic chain segment in the modifier has a strong interaction with the non-solvent in the coagulation bath. This strong interaction will lead to a strong exchange of solvents and non-solvents in the coagulation bath, so that the hydrophilic segments in the

modifier migrate to the surface of the membrane and enrich on the surface of the modified membrane to form a hydrophilic molecular brush. It also promotes the cross section of the membrane to produce wider finger-like pore structures. The hydrophilic molecular brush enriched on the membrane surface can significantly improve the hydrophilicity and anti-fouling performance of the modified membrane.

The surface hydrophilicity of the membranes estimated by means of water contact angle (WCA) is depicted in Fig. 8. It can be observed that the pristine PES membrane has a high
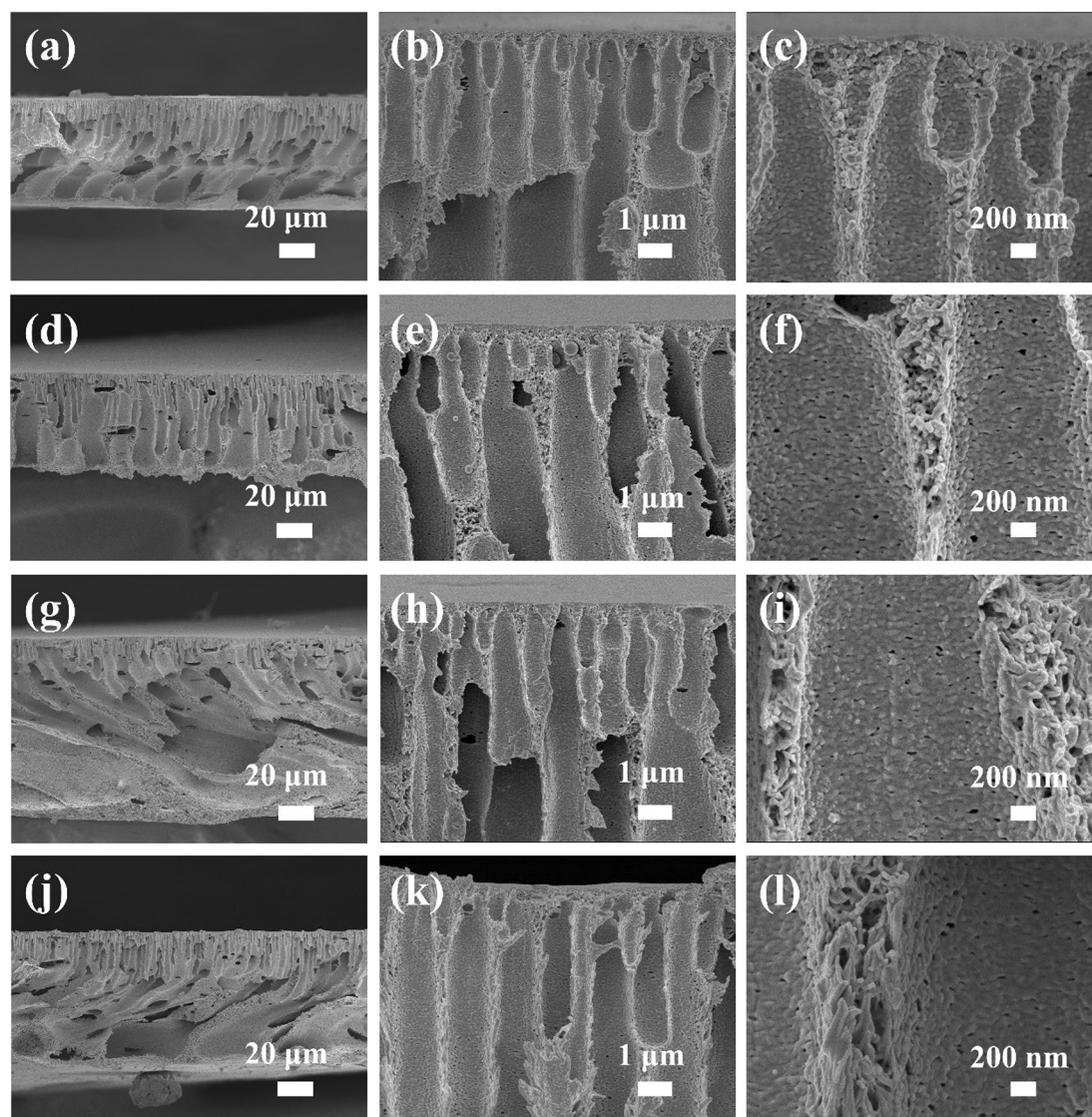
Figure 7: SEM images of cross-sectional views of membranes: (a, b, and c) M-PES, (d, e, and f) M-DexDTM-AuNP-1, (g, h, and i) M-DexDTM-AuNP-2, and (j, k, and l) M-DexDTM-AuNP-3.

WCA close to 90° due to the hydrophobicity nature of PES itself. In comparison with the pristine PES membrane, WCA of the DexDTM-AuNP-modified membrane significantly decreases. Moreover, WCA value of the modified membrane decreases with the increase of the amount of the DexDTM-AuNP. When the content of DexDTM-AuNP is 3 wt%, the WCA of the modified membrane decreases from 89.3° to 61.1°. The high hydrophilicity of the modified membrane is attributed to the excess of hydrophilic functional groups in DexDTM-AuNP such as -OH with higher hydrophilicity. In the phase inversion preparation of the modified membrane, there is a strong interaction between the hydrophilic segments in the additive and water molecules in the coagulation bath, which causes many hydrophilic segments to spontaneously migrate towards the membrane surface and increases its hydrophilicity.

It can be observed from the pure water fluxes of the membranes as shown in Fig. 9(a) that the pristine PES membrane has a low permeation flux, because of the hydrophobic nature of PES. In comparison with the pristine PES membrane, the pure water flux of the DexDTM-AuNP-modified membrane increases significantly and also increases with the increase of additive amount. From the figure, one can be found that the increase trend of pure water flux is well matched with the improvement of hydrophilicity, indicating that the increase of hydrophilicity is positively correlated with the flux of pure water. When the content of DexDTM-AuNP is 3 wt%, the pure water flux of the modified membrane is up to 134.5 L m^{-2} h^{-1}. Figure 9b records
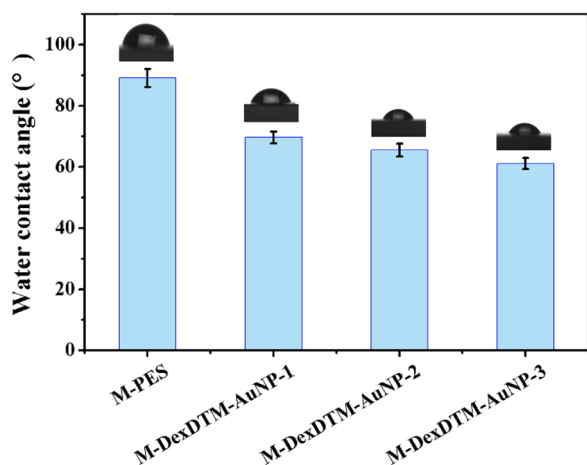
Figure 8: The average water contact angles on the top surface of membranes.

the time-dependent flux curves of water and BSA solutions for one recycles. It can be also found that the flux of the modified membrane has been significantly improved and increases with the increase of DexDTM-AuNP content. However, when the feed solution is changed from ultrapure water to BSA solution, the permeation flux of the membrane significantly reduces. The following two points can explain this phenomenon. On the one hand, BSA molecules block some pores on the surface of the membrane. On the other hand, the BSA molecule can increase the viscosity of water, and thus, reduces the permeability of the modified membrane. After rinsing the membrane contaminated with BSA for 1 h, the pure water flux test is performed again, and the pure water flux is almost completely restored to the initial state. The anti-fouling performance of membranes is shown in Fig. 9(c). The total fouling ratio (R_t) includes reversible fouling ratio (R_{ir}) and irreversible fouling ratio (R_r). Among them, the R_{ir} refers to that some pollutants adhering to the surface of the film cannot be cleaned down, while the R_r refers to that some pollutants with weak adhesion can be removed by cleaning. It
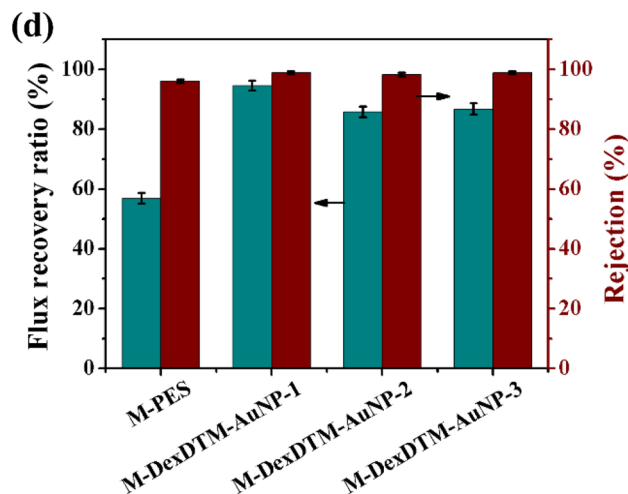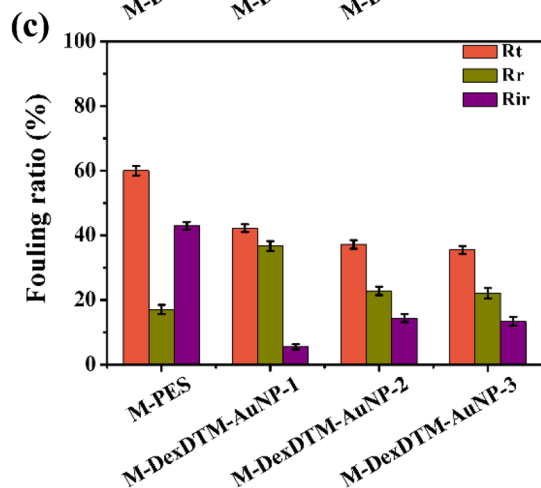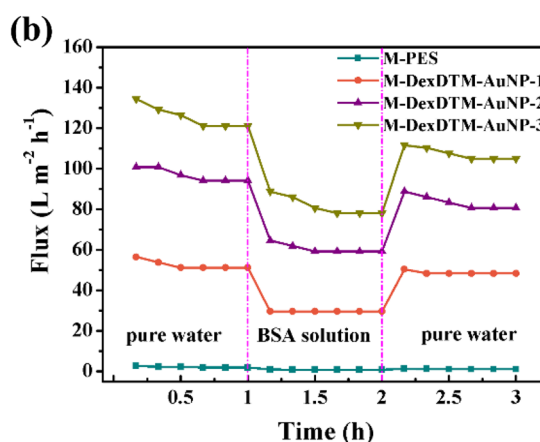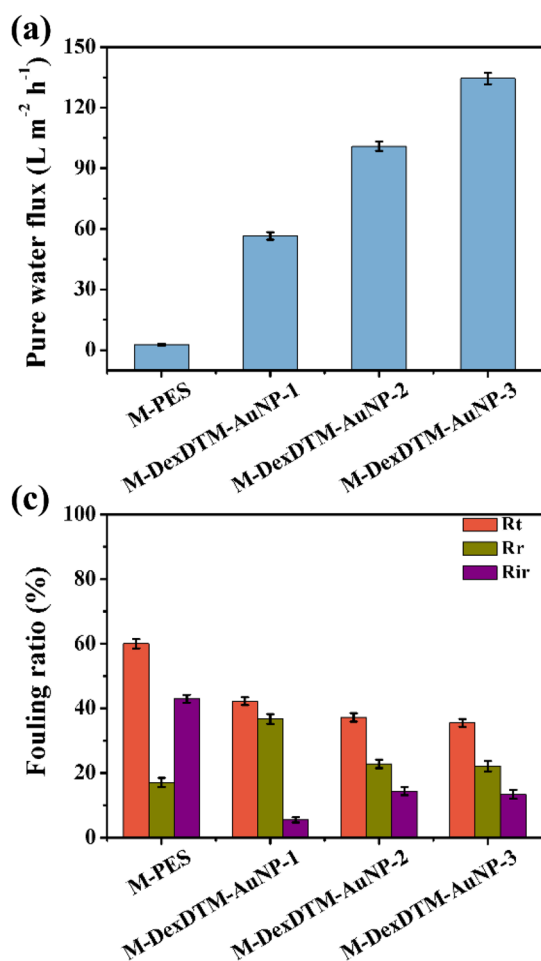
Figure 9: Properties of M-DexDTM-AuNP with contents of 1, 2, and 3 wt%: (a) pure water flux, (b) time-dependent fluxes, (c) fouling ratio, (d) flux recovery ratios (FRR), and BSA Rejections ratios.

can be observed that with the increase of additive content, the R_t of the modified membrane gradually decreased; the R_{ir} of the modified membrane gradually decreased and then increased slightly. However, the R_r of the modified membrane first increased and then decreased slightly. The main reason is that the hydrophilic groups on the membrane surface have strong interaction with water molecules, which can hinder BSA molecules and other fouling agents' adsorption on the membrane surface. Therefore, the excellent hydrophilicity would improve the membrane performance in terms of low fouling tendency and good water permeability. The flux recovery ratio (FRR) and BSA rejection ratio are shown in Fig. 9(d). Generally, the higher FRR indicates that the membrane has better anti-fouling performance. It can be observed that the FRR of the pristine PES membrane is only 56%. Compared with the pristine PES membrane, the FRR of the DexDTM-AuNP-modified membrane increases significantly, and FRR improves from 56 to 86%. This indicates that the DexDTM-AuNP-modified membrane has excellent anti-fouling properties. In addition, the BSA rejection ratio of the modified membrane also increased slightly compared to the pristine PES membrane, and the rejection ratio for BSA is always maintained above 98%. The above results indicate that the DexDTM-AuNP modified membrane has excellent permeability, anti-fouling, and BSA rejection properties.

The rejection performance of M-DexDTM-AuNP-3 for BSA, MB, and CR is shown in Fig. 10a. It can be seen from the figure that the rejection ratios of the modified membranes for BSA, CR, and MB are 98.8, 99.3, and 93.6%, respectively. The results show that the DexDTM-AuNP-modified membrane has excellent selective separation performance. The optical photographs of the CR, and MB solutions before and after filtrations are shown in Fig. 10b. From the optical photograph, it can be found that permeate of CR and MB changes significantly compared with the color of the feed solution, further indicating that the

modified membrane has an excellent separation performance. The above results show that the DexDTM-AuNP-modified membrane has great potential in industrial production fields, such as food processing, wastewater treatment, seawater desalination, etc.

Conclusions

In summary, the polysaccharide-functionalized gold nanoparticles (DexDTM-AuNP) was synthesized by one-step reduction with $NaBH_4$ and used as one novel additive to blend with PES to prepare ultrafiltration membranes via a non-solvent-induced phase separation technique. Compared with pristine PES membrane, the hydrophilicity of the DexDTM-AuNP-modified membrane was significantly improved. When the content of DexDTM-AuNP was 3 wt%, the WCA of the modified membrane decreases from 89.3° to 61.1°, and the pure water flux of the modified membrane has been increased up to 134.5 L m^{-2} h^{-1}. In addition, the modified membrane had high rejection ratios of BSA, CR and MB, which were 98.8, 99.3, and 93.6%, respectively, indicating that the DexDTM-AuNP-modified membrane had excellent hydrophilicity and rejection properties.

Experimental

Chemicals and materials

Polyethersulfone (PES, Ultrason E6020P, $Mw = 58,000$) was acquired from *BASF, Germany*. *N, N*-dimethylacetamide (DMAc, AR, 99.0%) was obtained from *Sino-pharm Chemical Reagent Co., Ltd, China,* and used as solvents. Chloroauric acid ($HAuCL_4$, AR) was purchased from *Nanjing Xianfeng Nanomaterials Technology Co., Ltd.*; 1-dodecanethiol ($C_{12}H_{26}S$, 98%), methyltrioctyl ammonium chloride (97%), dextran ($Mw \approx 70,000$), and 2-dimethylaminopyridine (97%) were
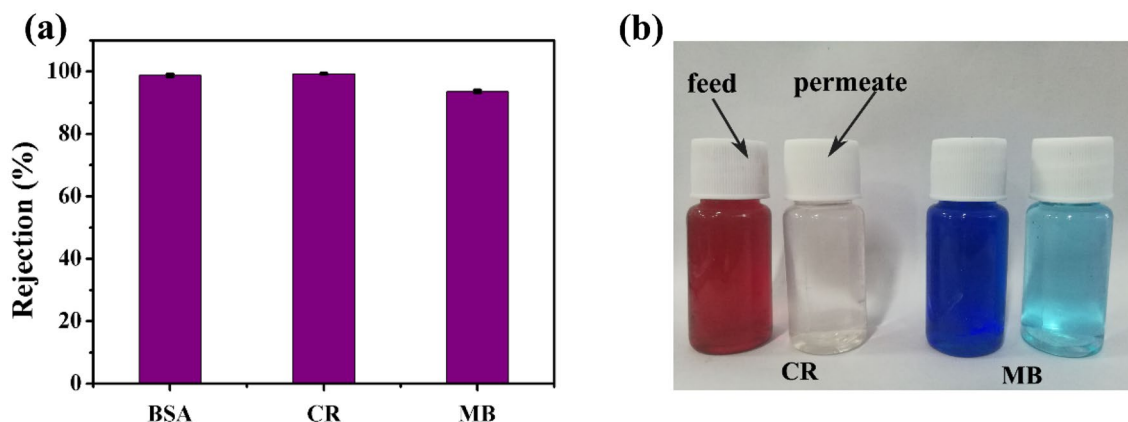
Figure 10: Separation properties of the DexDTM-AuNP-3 modified membranes: (a) rejection ratios of BSA, CR, and MB; and (b) optical photograph of the different dye solutions before and after filtration.

supplied by *Shanghai Macklin Biochemical Co., Ltd.* Sodium citrate (AR) was gained from *Sinopharm Chemical Reagent Co., Ltd.* Sodium hydroxide (NaOH, AR) and *n*-hexane were bought from *Tianjin Baishi Chemical Co., Ltd.* Sodium borohydride (NaBH$_4$, AR) was purchased from *Shanghai Zhongtai Chemical Reagent Co., Ltd.* Bovine serum albumin (BSA), congo red (CR), and methyl blue (MB) were provided by *Aladdin Reagent.* Carbon disulfide (CS$_2$, AR) was acquired from *Chengdu Cologne Chemical Co., Ltd.* Hydrochloric acid (HCl, 37%) was purchased from *Guo Yao Chemical Reagent Company.* All other reagents (analytical grade) were obtained from *Sinopharm Chemical Reagent Co., Ltd, China*, and used without further purification. Ultrapure water was made in laboratory.

Preparation of RAFT agents (DTM)

1-dodecythiol (12 mL), acetone (40 mL), and methyltrioctyl ammonium chloride (0.8 mL) were mixed in a three-necked round bottom flask under the atmosphere of N$_2$, and the temperature of the solution was controlled at 5–10 °C with ice-water bath. After bubbling with N$_2$ for 30 min, a 50% NaOH solution (4 mL) was added dropwise to the mixture, and the reaction mixture was allowed to proceed at N$_2$ atmosphere and stirred for 20 min; carbon disulfide (3 mL) was mixed in acetone (8 mL) and added dropwise to the solution, the reaction was stirred for an additional 30 min; after adding chloroform (4.5 mL) to the solution at one time, followed by the addition of a 50% NaOH solution (13 mL) drop by drop, and the reaction continued at room temperature for 12 h. The crude product was obtained by adding ultrapure water (65 mL) and concentrated HCl (33 mL) to the solution. The crude product was recrystallized from *n*-hexane, so 2-(dodecylthiocarbonothioylthio)-2-methylpropanoic acid (DTM) was finally synthesized.

Synthesis of dextran-based macro-chain transfer agent (DexDTM)

First, DTM (0.55 g) was dissolved in dichloromethane (5 mL) at room temperature, and oxalyl chloride (1.5 g) was added to the solution under N$_2$ protection. Then the reaction was carried out under stirring at 50 °C for 2 h, dextran (1.0 g), 2-dimethylaminopyridinium (0.38 g), and triethylamine (0.31 g) were thoroughly mixed in dimethyl sulfoxide (10 mL) and added to the mixture. The reaction was continued at 80 °C for 24 h, and then ethanol was added to precipitate. The precipitated solid was washed several times with ethanol and centrifuged to obtain a pale yellow solid. Finally, DexDTM was obtained via esterification of DTM with dextran hydroxyl group.

Self-assembly of dextran on gold nanoparticles

The functionalized gold nanoparticles were prepared by one-step reduction with NaBH$_4$. The specific experimental steps are as follows: 0.25 g of DexDTM was dissolved in 100 mL of deionized water under N$_2$ protection, and 10 mL of HAuC1$_4$ solution (4 mg mL^{-1}) was added to the mixture. After continuous stirring in an ice-water bath for 30 min, 10 mL trisodium citrate (10 mg mL^{-1}), and 10 mL NaBH$_4$ solution (1.1 mg mL^{-1}) were added to the mixture in this order. The color of the solution changed immediately, and the reduction reaction continued at room temperature for 3 h. After completion of reaction, the resulting solution was freeze-dried and functional gold nanoparticles (DexDTM-AuNP) were obtained.

Preparation of membranes

The modified membranes were prepared via the non-solvent-induced phase separation (NIPS) method. In details, a certain mass fraction of DexDTM-AuNP was added into DMAc. After DexDTM-AuNP was completely ultrasonic dispersed, a certain mass fraction of PES was then added into the mixture, which was stirred at room temperature for 12 h to form a homogeneous solution. The casting solution was then degassed for 1 h at room temperature and coated on a clean glass surface, followed by spin casting and immersed in the coagulation bath for precipitation at room temperature to form the DexDTM-AuNP-modified membranes. Finally, the synthesized membranes were repeatedly rinsed with ultrapure water to remove residual solvent and dried at 40 °C for 24 h. In this study, the prepared PES membranes containing 0, 1, 2, and 3 wt% DexDTM-AuNP are named as M-PES, M-DexDTM-AuNP-1, M-DexDTM-AuNP-2, and M-DexDTM-AuNP-3, respectively.

Characterizations

The chemical structure of the additive (DexDTM and DexDTM-AuNP) and the functional groups on the surface of membranes were characterized using a FTIR Nexus 670 (Nicolet American) instrument and an H-NMR spectrometer FT-80 (Varian American). The morphologies of the prepared DexDTM-AuNP were observed by transmission electron microscopy (TEM, TECNAI TF20). DexDTM-AuNP was ultrasonically dispersed in absolute ethanol and then dropped on a micro-bashan mesh with a supporting film. After the liquid evaporating, the samples were observed by TEM. The surface chemical compositions of the membranes were investigated by X-ray photoelectron spectroscopy (XPS, XSAM800, KRATOS Co., Britain). The top surface and cross-sectional morphologies of the membrane were characterized by field emission scanning electron microscopy (FE-SEM, JSM-6700F JEOL, *Japan*). Based on the principle of

secondary electron imaging, field emission scanning electron microscopy (SEM) can observe the microstructure of the sample at the nanoscale under low voltage and obtain the ultrastructure information of the sample surface with strong three-dimensional sense. The membrane were fractured in liquid nitrogen to obtain their cross-sectional structure. Conductive glue was used to adhere the surface and section of the membrane to the copper column and then deposit a layer of gold on the surface of the sample with a vacuum coater to improve the conductivity of the polymer membrane. Then use the FE-SEM to observe the surface and cross-sectional topography. The wettability of the membranes was investigated by the contact angle analyzer (WCA, PHS-3C, *Precision Science Co., Shanghai, China*) at room temperature [41–43].

Membrane performance test

The performance of the membranes, including permeation flux, anti-fouling ability, water recovery ratio, and BSA/dye rejection, was investigated in a cross-flow filtration setup with a membrane effective surface area of 23.7 cm^2. All the experiments were conducted at a pressure of 0.2 MPa, and the data of flux were recorded every 10 min. Before measurement, the membrane was pre-compacted for 30 min to obtain a steady permeation flux. The rejection performance of membrane was performed using BSA aqueous solutions (1 g L^{-1}), CR solution (250 mg mL^{-1}), and MB solution (250 mg mL^{-1}). All the calculation formulas are used in this article according to our previous work [41, 44].

Data availability

Data generated during the study are subject to a data sharing mandate and available in a public repository that does not issue datasets with DOIs.

References

1. L. Zhu, L. Zhu, J. Jiang, Z. Yi, Y. Zhao, B. Zhu, Y. Xu, Hydrophilic and anti-fouling polyethersulfone ultrafiltration membranes with poly(2-hydroxyethyl methacrylate) grafted silica nanoparticles as additive. J. Membr. Sci. **451**, 157–168 (2014)

2. K. Zhu, S. Zhang, J. Luan, Y. Mu, Y. Du, G. Wang, Fabrication of ultrafiltration membranes with enhanced antifouling capability and stable mechanical properties via the strategies of blending and crosslinking. J. Membr. Sci. **539**, 116–127 (2017)

3. J. Zhu, Q. Zhang, J. Zheng, S. Hou, H. Mao, S. Zhang, Green fabrication of a positively charged nanofiltration membrane by grafting poly(ethylene imine) onto a poly (arylene ether sulfone) membrane containing tertiary amine groups. J. Membr. Sci. **517**, 39–46 (2016)

4. W. Zhong, J. Hou, H. Yang, V. Chen, Superhydrophobic membranes via facile bio-inspired mineralization for vacuum membrane distillation. J. Membr. Sci. **540**, 98–107 (2017)

5. Y. Zhao, L. Zhu, Z. Yi, B. Zhu, Y. Xu, Zwitterionic hydrogel thin films as antifouling surface layers of polyethersulfone ultrafiltration membranes anchored via reactive copolymer additive. J. Membr. Sci. **470**, 148–158 (2014)

6. J. Zhang, Z. Xu, W. Mai, C. Min, B. Zhou, M. Shan, Y. Li, C. Yang, Z. Wang, X. Qian, Improved hydrophilicity, permeability, antifouling and mechanical performance of PVDF composite ultrafiltration membranes tailored by oxidized low-dimensional carbon nanomaterials. J. Mater. Chem. A **1**, 3101–3111 (2013)

7. D. Zhang, A. Karkooti, L. Liu, M. Sadrzadeh, T. Thundat, Y. Liu, R. Narain, Fabrication of antifouling and antibacterial polyethersulfone (PES)/cellulose nanocrystals (CNC) nanocomposite membranes. J. Membr. Sci. **549**, 350–356 (2018)

8. H. Zangeneh, A. Zinatizadeh, S. Zinadini, M. Feyzi, D. Bahnemann, Preparation and characterization of a novel photocatalytic self-cleaning PES nanofiltration membrane by embedding a visible-driven photocatalyst boron doped-TiO$_2$-SiO$_2$/CoFe$_2$O$_4$ nanoparticles. Sep. Purif. Technol. **209**, 764–775 (2019)

9. H. Zangeneh, A. Zinatizadeh, S. Zinadini, M. Feyzi, D.W. Bahnemann, A novel photocatalytic self-cleaning PES nanofiltration membrane incorporating triple metal-nonmetal doped TiO2 (K-B-N-TiO2) for post treatment of biologically treated palm oil mill effluent. React. Funct. Polym. **127**, 139–152 (2018)

10. H. Zangeneh, A. Zinatizadeh, M. Feyzi, S. Zinadini, D. Bahnemann, Photomineralization of recalcitrant wastewaters by a novel magnetically recyclable boron doped-TiO$_2$-SiO$_2$ cobalt ferrite nanocomposite as a visible-driven heterogeneous photocatalyst. J. Environ. Chem. Eng. **6**, 6370–6381 (2018)

11. F. Yang, F. Tao, C. Li, L. Gao, P. Yang, Self-assembled membrane composed of amyloid-like proteins for efficient size-selective molecular separation and dialysis. Nat. Commun. **9**, 5443 (2018)

12. Q. Xue, H. Cao, F. Meng, M. Quan, Y. Gong, Cell membrane mimetic coating immobilized by mussel-inspired adhesion on commercial ultrafiltration membrane to enhance antifouling performance. J. Membr. Sci. **528**, 1–11 (2017)

13. Z. Xu, J. Liao, H. Tang, J. Efome, N. Li, Preparation and antifouling property improvement of tröger's base polymer ultrafiltration membrane. J. Membr. Sci. **561**, 59–68 (2018)

14. C. Xu, X. Liu, B. Xie, C. Yao, W. Hu, Y. Li, X. Li, Preparation of PES ultrafiltration membranes with natural amino acids based zwitterionic antifouling surfaces. Appl. Surf. Sci. **385**, 130–138 (2016)

15. Y. Wu, S. Xu, T. Wang, C. Wang, Enhanced metal ion rejection by a low-pressure microfiltration system using cellulose filter papers modified with citric acid. ACS Appl. Mater. Interfaces. **10**, 32736–32746 (2018)

16. R. Wei, F. Yang, R. Gu, Q. Liu, J. Zhou, X. Zhang, W. Zhao, C. Zhao, Design of robust thermal and anion dual-responsive membranes with switchable response temperature. ACS Appl. Mater. Interfaces. **10**, 36443–36455 (2018)

17. Z. Wang, Z. Wang, S. Lin, H. Jin, S. Gao, Y. Zhu, J. Jin, Nanoparticle-templated nanofiltration membranes for ultrahigh performance desalination. Nat. Commun. **9**, 2004 (2018)

18. Y. Wang, J. Zhu, G. Dong, Y. Zhang, N. Guo, J. Liu, Sulfonated halloysite nanotubes/polyethersulfone nanocomposite membrane for efficient dye purification. Sep. Purif. Technol. **150**, 243–251 (2015)

19. J. Wang, S. Zhang, P. Wu, W. Shi, Z. Wang, Y. Hu, In situ surface modification of thin-film composite polyamide membrane with zwitterions for enhanced chlorine resistance and transport properties. ACS Appl. Mater. Interfaces. **11**, 12043–12052 (2019)

20. B. Wang, J. Ji, K. Li, Crystal nuclei templated nanostructured membranes prepared by solvent crystallization and polymer migration. Nat. Commun. **7**, 12804 (2016)

21. C. Sun, X. Feng, Enhancing the performance of PVDF membranes by hydrophilic surface modification via amine treatment. Sep. Purif. Technol. **185**, 94–102 (2017)

22. H. Song, F. Ran, H. Fan, X. Niu, L. Kang, C. Zhao, Hemocompatibility and ultrafiltration performance of surface-functionalized polyethersulfone membrane by blending comb-like amphiphilic block copolymer. J. Membr. Sci. **471**, 319–327 (2014)

23. F. Ran, J. Wu, X. Niu, D. Li, C. Nie, R. Wang, W. Zhao, W. Zhang, Y. Chen, C. Zhao, A new approach for membrane modification based on electrochemically mediated living polymerization and self-assembly of n-tert-butyl amide- and beta-cyclodextrin-involved macromolecules for blood purification. Mater. Sci. Eng., C **95**, 122–133 (2019)

24. S. Zhang, Qi. Wang, D. Li, F. Ran, Single-walled carbon nanotubes grafted with dextran as additive to improve separation performance of polymer membranes. Sep. Purif. Technol. **254**, 117584 (2021)

25. M. Abidin, P. Goh, A. Ismail, M. Othman, H. Hasbullah, N. Said, S. Kadir, F. Kamal, M. Abdullah, B. Ng, Antifouling polyethersulfone hemodialysis membranes incorporated with poly (citric acid) polymerized multi-walled carbon nanotubes. Mater. Sci. Eng., C **68**, 540–550 (2016)

26. T. Cai, X. Li, C. Wan, T. Chung, Zwitterionic polymers grafted poly(ether sulfone) hollow fiber membranes and their antifouling behaviors for osmotic power generation. J. Membr. Sci. **497**, 142–152 (2016)

27. C. Chen, J. Wang, D. Liu, C. Yang, Y. Liu, R. Ruoff, W. Lei, Functionalized boron nitride membranes with ultrafast solvent transport performance for molecular separation. Nat. Commun. **9**, 1902 (2018)

28. D. Davenport, J. Lee, M. Elimelech, Efficacy of antifouling modification of ultrafiltration membranes by grafting zwitterionic polymer brushes. Sep. Purif. Technol. **189**, 389–398 (2017)

29. X. Du, Z. Wang, W. Liu, J. Xu, Z. Chen, C. Wang, Imidazolium-functionalized poly (arylene ether ketone) cross-linked anion exchange membranes. J. Membr. Sci. **566**, 205–212 (2018)

30. M. Esfahani, S. Aktij, Z. Dabaghian, M. Firouzjaei, A. Rahimpour, J. Eke, I. Escobar, M. Abolhassani, L. Greenlee, A. Esfahani, A. Sadmani, N. Koutahzadeh, Nanocomposite membranes for water separation and purification: Fabrication, modification, and applications. Sep. Purif. Technol. **213**, 465–499 (2019)

31. M. Esfahani, N. Koutahzadeh, A. Esfahani, M. Firouzjaei, B. Anderson, L. Peck, A novel gold nanocomposite membrane with enhanced permeation, rejection and self-cleaning ability. J. Membr. Sci. **573**, 309–319 (2019)

32. A. Giwa, S. Chakraborty, M. Mavukkandy, H. Arafat, S. Hasan, Nanoporous hollow fiber polyethersulfone membranes for the removal of residual contaminants from treated wastewater effluent: Functional and molecular implications. Sep. Purif. Technol. **189**, 20–31 (2017)

33. M. Haase, H. Jeon, N. Hough, J. Kim, K. Stebe, D. Lee, Multifunctional nanocomposite hollow fiber membranes by solvent transfer induced phase separation. Nat. Commun. **8**, 1234 (2017)

34. M. He, K. Gao, L. Zhou, Z. Jiao, M. Wu, J. Cao, X. You, Z. Cai, Y. Su, Z. Jiang, Zwitterionic materials for antifouling membrane surface construction. Acta Biomater. **40**, 142–152 (2016)

35. H. Ji, C. He, R. Wang, X. Fan, L. Xiong, W. Zhao, C. Zhao, Multifunctionalized polyethersulfone membranes with networked submicrogels to improve antifouling property, antibacterial adhesion and blood compatibility. Mater. Sci. Eng., C **96**, 402–411 (2019)

36. A. Khan, T. Sherazi, Y. Khan, S. Li, S. Naqvi, Z. Cui, Fabrication and characterization of polysulfone/modified nanocarbon black composite antifouling ultrafiltration membranes. J. Membr. Sci. **554**, 71–82 (2018)

37. I. Kolesnyk, V. Konovalova, K. Kharchenko, A. Burban, K. Knozowska, W. Kujawski, J. Kujawa, Improved antifouling properties of polyethersulfone membranes modified with α-amylase entrapped in tetronic micelles. J. Membr. Sci. **570–571**, 436–444 (2019)

38. Y. Lin, C.H. Loh, L. Shi, Y. Fan, R. Wang, Preparation of high-performance Al_2O_3/PES composite hollow fiber UF membranes via facile in-situ vapor induced hydrolyzation. J. Membr. Sci. **539**, 65–75 (2017)

39. O. Mahlangu, R. Nackaerts, J. Thwala, B. Mamba, A. Verliefde, Hydrophilic fouling-resistant GO-ZnO/PES membranes for wastewater reclamation. J. Membr. Sci. **524**, 43–55 (2017)

40. M. Mavukkandy, Q. Zaib, H. Arafat, CNT/PVP blend PVDF membranes for the removal of organic pollutants from simulated treated wastewater effluent. J. Environ. Chem. Eng. **6**, 6733–6740 (2018)

41. D. Li, X. Niu, S. Yang, Y. Chen, F. Ran, Thermo-responsive polysulfone membranes with good anti-fouling property modified by grafting random copolymers via surface-initiated eATRP. Sep. Purif. Technol. **206**, 166–176 (2018)

42. M.K. Ahn, B. Lee, J. Jang, C.M. Min, S.B. Lee, C. Pak, J. Lee, Facile preparation of blend proton exchange membranes with highly sulfonated poly(arylene ether) and poly(arylene ether sulfone) bearing dense triazoles. J. Membr. Sci. **560**, 58–66 (2018)

43. I. Abdulazeez, A. Matin, M. Khan, M.M. Khaled, M.A. Ansari, S. Akhtar, S. Rehman, Facile preparation of antiadhesive and biocidal reverse osmosis membranes using a single coating for efficient water purification. J. Membr. Sci. **591**, 117299 (2019)

44. S. Zhang, Y. Liu, D. Li, Q. Wang, F. Ran, Water-soluble MOF nanoparticles modified polyethersulfone membrane for improving flux and molecular retention. Appl. Surf. Sci. **505**, 144553 (2020)